

Administration of rhIL-7 in humans increases in vivo TCR repertoire diversity by preferential expansion of naive T cell subsets

Claude Sportès,¹ Frances T. Hakim,¹ Sarfraz A. Memon,¹ Hua Zhang,²
 Kevin S. Chua,² Margaret R. Brown,⁴ Thomas A. Fleisher,⁴
 Michael C. Krumlauf,¹ Rebecca R. Babb,¹ Catherine K. Chow,³
 Terry J. Fry,² Julie Engels,⁵ Renaud Buffet,⁵ Michel Morre,⁵
 Robert J. Amato,⁶ David J. Venzon,⁷ Robert Korngold,⁸ Andrew Pecora,⁸
 Ronald E. Gress,¹ and Crystal L. Mackall²

¹Experimental Transplantation and Immunology Branch; ²Pediatric Oncology Branch, Center for Cancer Research, National Cancer Institute; ³Departments of Radiology; ⁴Department of Laboratory Medicine, Clinical Center, National Institutes of Health, Bethesda, MD 20892

⁵Cytheris Inc., Rockville, MD 20850

⁶Methodist Hospital, Texas Medical Center, Houston, TX 77021

⁷Biostatistics and Data Management Section, National Cancer Institute; ⁸The Cancer Center at Hackensack University Medical Center, Hackensack, NJ 07601

Interleukin-7 (IL-7) is a homeostatic cytokine for resting T cells with increasing serum and tissue levels during T cell depletion. In preclinical studies, IL-7 therapy exerts marked stimulating effects on T cell immune reconstitution in mice and primates. First-in-human clinical studies of recombinant human IL-7 (rhIL-7) provided the opportunity to investigate the effects of IL-7 therapy on lymphocytes *in vivo*. rhIL-7 induced *in vivo* T cell cycling, bcl-2 up-regulation, and a sustained increase in peripheral blood CD4⁺ and CD8⁺ T cells. This T cell expansion caused a significant broadening of circulating T cell receptor (TCR) repertoire diversity independent of the subjects' age as naive T cells, including recent thymic emigrants (RTEs), expanded preferentially, whereas the proportions of regulatory T (T reg) cells and senescent CD8⁺ effectors diminished. The resulting composition of the circulating T cell pool more closely resembled that seen earlier in life. This profile, distinctive among cytokines under clinical development, suggests that rhIL-7 therapy could enhance and broaden immune responses, particularly in individuals with limited naive T cells and diminished TCR repertoire diversity, as occurs after physiological (age), pathological (human immunodeficiency virus), or iatrogenic (chemotherapy) lymphocyte depletion.

CORRESPONDENCE

Claude Sportès:
 cspories@mail.nih.gov

Abbreviations used: CT, computerized tomography; γc, common γ chain; rh, recombinant human; MFI, mean fluorescence intensity; RTE, recent thymic emigrant; TREC, TCR excision circle.

Cytokines that signal via the common γ chain (γc) represent promising therapeutics based on their potential to augment T cell expansion and increase the effectiveness of immune-based therapies (1–6). Within this family, IL-2 is a prototypic activating cytokine, secreted by and selectively signaling activated T cells, as well as up-regulating its own receptor (IL-2R). In contrast, IL-7 is a prototypic homeostatic cytokine, produced constitutively by nonlymphoid cells. Its receptor (IL-7Rα) is expressed on resting T cells, and then rapidly down-regulated

after T cell activation or IL-7 signaling (7). IL-7 is essential for T cell development in mice (8–10) and humans (11, 12), as well as for T cell homeostasis, because it is required to maintain naive CD4⁺ and CD8⁺ T cells *in vivo* (13, 14). IL-7 levels rise in serum and tissues after T cell depletion and fall upon recovery (14–16).

In preclinical studies, IL-7 therapy exerts marked effects on T cell immune reconstitution in mice (17) and primates (18–20). IL-7 augments effector and memory responses to vaccination in mice (21) with preferential enhancement of responses to weak subdominant antigens. In preclinical models, IL-7 therapy

R.E. Gress and C.L. Mackall contributed equally to this paper.
 The online version of this article contains supplemental material.

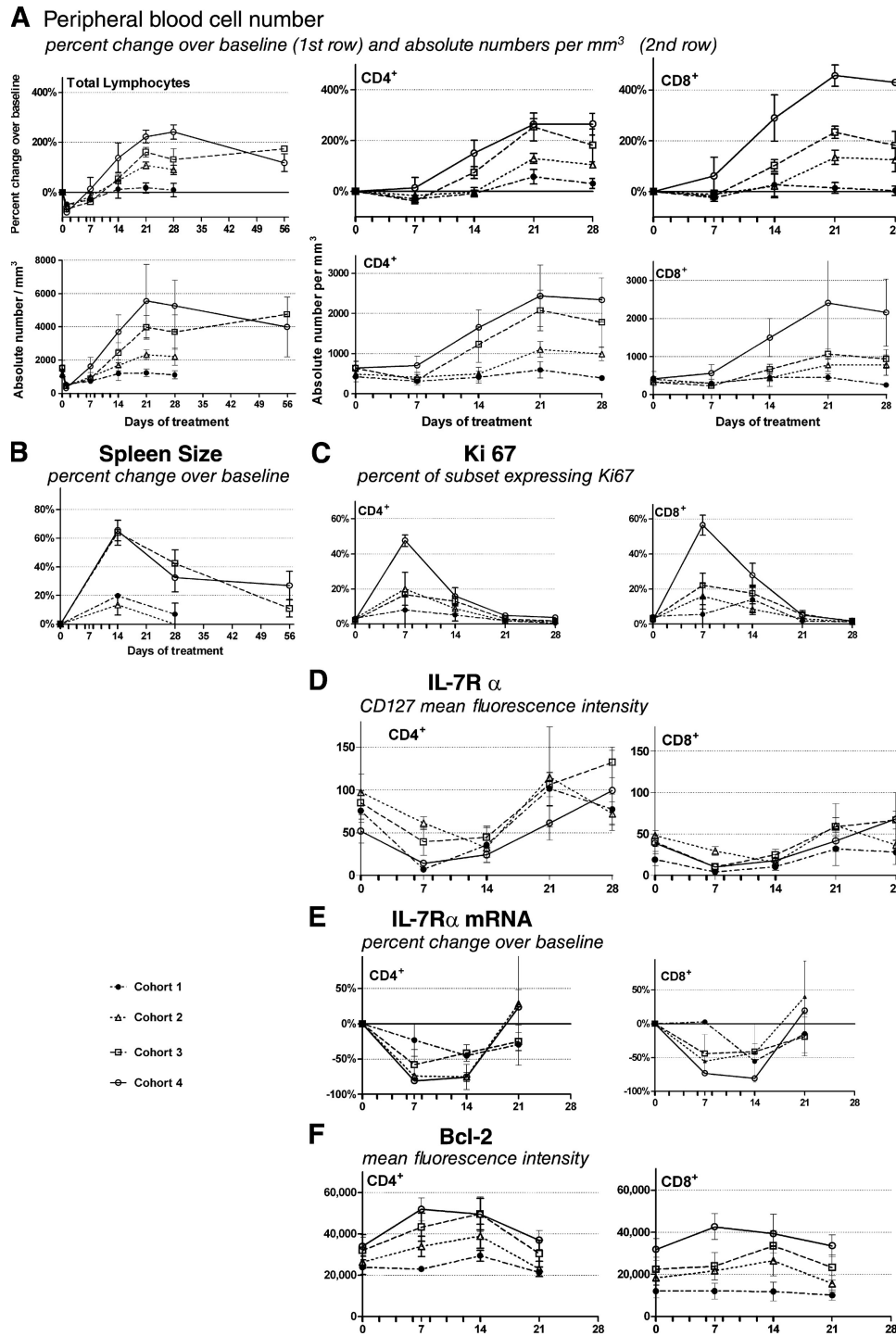


Figure 1. Effects of rhIL-7 therapy on circulating T cells and spleen. rhIL-7 was administered every other day on day 1–14 (8 injections, indicated by tick marks on X axis), at 4 dose levels: 3 $\mu\text{g}/\text{kg}/\text{d}$ (dashed line with ●; $n = 3$); 10 $\mu\text{g}/\text{kg}/\text{d}$ (dotted line with △; $n = 3$); 30 $\mu\text{g}/\text{kg}/\text{d}$ (dashed line with □; $n = 5$); and 60 $\mu\text{g}/\text{kg}/\text{d}$ (solid line with ○; $n = 4$). Mean value for each cohort (\pm the SEM) are plotted at the indicated time points. (A) The absolute lymphocyte count from complete blood counts (left) and flow cytometry-based frequency were used to determine circulating absolute CD3+/CD4+ and CD3+/CD8+ counts, absolute numbers \pm the SEM (bottom graphs), and percent change in absolute numbers over baseline (top graphs) of the respective subsets shown on day 1 (total lymphocytes only), 7, 14, 21, and 28 for all treated subjects, as well as day 55–90 for subjects treated with 30 or 60 $\mu\text{g}/\text{kg}/\text{d}$. Baseline values represent the mean of four separate analyses performed in each subject within 2 wk before initiation of rhIL-7 therapy. (B) Spleen size: bidimensional product by CT scan obtained at the time points shown; percent changes from the pretherapy scan are plotted. (C–F) Baseline (1 value obtained on day 0) and day 7, 14, 21, and 28 data points were generated for CD3+/CD4+ (left) and CD3+/CD8+ subsets (right). (C) Ki-67 shows the percentage of cells in the respective subsets expressing Ki-67 via flow cytometry at the time points shown. (D) IL-7R α expression

augments antitumor responses, leading to improved survival when combined with antitumor vaccines (21, 22). The capacity for supranormal levels of IL-7 to augment T cell cycling in response to antigens with low affinity for the TCR appears largely responsible for homeostatic peripheral expansion, which involves increased T cell proliferation to self-antigens during lymphopenia (13, 23, 24). Many studies have documented a central role for homeostatic peripheral expansion in the immunorestorative effect of IL-7 therapy (19, 20, 25), whereas augmentation of thymic output has also been recently suggested (18). In regard to CD4⁺CD25^{Hi} regulatory T (T reg) cells, IL-2 plays a major role in their development, maintenance, and expansion, whereas T reg cells express low IL-7R α levels (26, 27) and recent work suggests that IL-7 therapy can expand CD4⁺ T cells without expanding T reg cells (28).

Lymphopenia induced by cytotoxic chemotherapy or other insults can significantly diminish immune function (29). In adults, CD4⁺ T cell recovery after severe immune depletion requires the reemergence of a pool of naive T cells, which requires 18–24 mo and may occur only in individuals younger than 40–45 yr (30, 31). A therapeutic approach to accelerate, or simply promote in older individuals, the recovery of a widely diverse T cell repertoire may find a multitude of clinical applications. If rhIL-7 therapy in humans can augment immune responses to weak antigens, hasten reconstitution of naive T cell populations, and spare T reg cell expansion in particular but not restricted to older individuals, it could improve the effectiveness of immune-based therapies for cancer or chronic infection in various populations with iatrogenic (chemotherapy), pathological (HIV), or physiological (aging) immune insufficiency. This study sought to characterize the immunobiologic effects of rhIL-7 therapy in humans and, specifically, its potential for immune rejuvenation of T cell subpopulations.

RESULTS

IL-7 therapy induces widespread T cell cycling and expands the T cell pool in humans in a dose-dependent manner, while preserving T cell function

To assess effects of IL-7 therapy on human lymphocytes *in vivo*, 16 subjects with refractory cancer (age 20–71) were enrolled on a phase I dose escalation trial of rhIL-7. Doses extrapolated from mouse and primate studies (3, 10, 30, and 60 μ g/kg) were administered subcutaneously every other day for 14 d (8 doses). As shown in Fig. 1 A, after a very transient decrease, circulating numbers of lymphocytes and CD4⁺ and CD8⁺ T cells increased in a dose-dependent manner, with increases at the highest dose level approaching 300% for CD4⁺ and exceeding 400% for CD8⁺ T cells. The initial decrease in circulating lymphocytes is likely caused by early trafficking out of the circulation and is also seen with administration of IL-2 and, more recently, IL-21. Specifically, we have observed by

FACS analysis an initial up-regulation of CXCR4 on circulating lymphocytes with rhIL-7 treatment (unpublished data), providing one plausible mechanism for T cell trafficking into SDF-1-rich tissues.

The degree of lymphocyte expansion showed no significant relationship to age (Fig. S1 B, available at <http://www.jem.org/cgi/content/full/jem.20071681/DC1>) and reflected increases in total body lymphocytes rather than sole trafficking of lymphocytes from lymphoid tissues into the bloodstream because they coincided with spleen (Fig. 1 B) and lymph node enlargement observed by computerized tomography (CT) scan and increased metabolic activity on positron emission tomography (PET)-CT on day 14 (Fig. 2). T cell numbers peaked 2 wk after the peak in cycling frequency (Fig. 1, A and C), and total lymphocyte numbers remained elevated for up to 6 wk after cessation of therapy (Fig. 1 A). Additionally, peripheral blood CD3 γ δ and CD3⁺/CD16⁺ T cells increased to a similar extent as $\alpha\beta$ T cells, whereas NK cells increased minimally at the two highest dose levels. Circulating B cells decreased during rhIL-7 therapy (Fig. S1 A). Pharmacologic serum levels of IL-7 were achieved in a dose-dependent manner documented on both the first and last day of treatment (Fig. S1 C). The lower serum levels achieved on the last day most likely reflects the much higher lymphocyte mass on that day. 5 out of 15 evaluable subjects developed anti-rhIL-7 antibodies at day 28 or 35, but importantly, none developed neutralizing antibodies as measured in a bioassay using an IL-7-dependent cell line, and no subject developed lymphopenia after treatment.

rhIL-7 therapy in primates augmented T cell cycling *in vivo* (19). To evaluate the effects of rhIL-7 therapy on T cell cycling in humans, we quantitated Ki-67 expression in total circulating CD4⁺ and CD8⁺ T cells before, during, and after IL-7 therapy (Fig. 1 C). At baseline, 1–3% of CD4⁺ and CD8⁺ cells expressed Ki-67, but a dose-dependent increase in cycling frequency was seen within 7 d of rhIL-7 initiation such that >40% of CD4⁺ T cells and >50% of CD8⁺ T cells expressed Ki-67 in subjects treated at the highest dose level. The time course of rhIL-7's effects on cell cycling was substantially influenced by dynamic regulation of IL-7R α expression. Despite continued administration of rhIL-7 through day 14 resulting in sustained increases in circulating IL-7 levels (Fig. S1 C), T cell cycling substantially declined after day 7 coincident with IL-7R α down-regulation (Fig. 1 D) that, as in mouse models (7), did not simply reflect receptor blockade or internalization because it was associated with diminished mRNA transcription (Fig. 1 E).

Like other γ c cytokines, IL-7 also supports T cell survival by up-regulating members of the antiapoptotic bcl-2 family (32, 33), and rhIL-7 therapy induced significant increases in T cell bcl-2 expression in this study (Fig. 1 F); as bcl-2 has

as MFI via flow cytometry for each subset. (E) IL-7R α mRNA expression represented as mean percent change from baseline of IL-7-R α mRNA copies normalized/10⁴ copies of AXTB via Q-PCR in sorted CD4⁺ and CD8⁺ cells. (F) bcl-2 expression as MFI (after subtracting background staining for each subset) via flow cytometry for each subset.

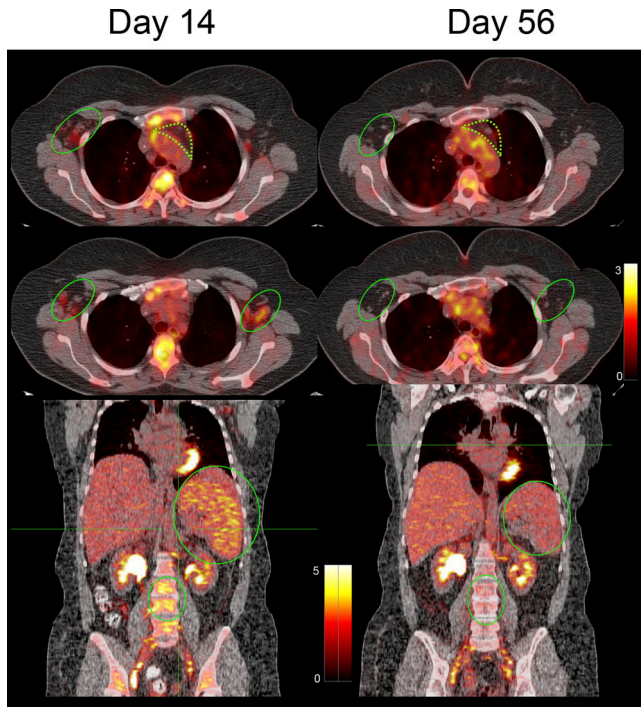


Figure 2. PET-CT imaging of the self-limited lymphoid organs' enlargement and increased metabolic activity after rhIL-7 therapy. Shown are representative images on PET-CT scan in one subject (42-yr-old female treated with 60 $\mu\text{g}/\text{kg}/\text{dose}$). (left) Imaging on day 14 (last day of rhIL-7 treatment). (right) Day 56 (6 wk after the end of treatment). The full ovals indicate areas of increased size (except for vertebral bodies) and activity of lymphoid organs (left and right axillary adenopathy, spleen, and lumbar spine) at the end of treatment. The dotted contours indicate the thymic area where no increased activity can be demonstrated at day 14. Increased metabolic activity is seen in pink and maximal in yellow areas.

been well established in animal studies to diminish programmed cell death, this rise in bcl-2 expression may have contributed mechanistically to the increase in T cell numbers. Whereas cell cycling rates were tightly linked to IL-7R α expression, bcl-2 up-regulation was sustained throughout therapy. At higher dose levels, bcl-2 expression persisted above baseline for at least 1 wk after discontinuation of rhIL-7 therapy. This sustained increase in bcl-2 expression was likely to be physiologically significant and contributed to the sustained increases in lymphocyte number observed, as similar effects have been seen in animals when sustained bcl-2 expression is induced.

To assess functionality of rhIL-7-expanded T cells, proliferation in response to TCR signaling in vitro was measured using titrated doses of plate-bound anti-CD3 (Fig. 3 A). rhIL-7 therapy substantially increased maximal T cell proliferation, which peaked on day 14, the last day of therapy. Proliferative responses to fully mitogenic doses of anti-CD3 were approximately threefold greater than at baseline and, at very low doses of anti-CD3 stimulation, rhIL-7-treated subjects showed increases in proliferation greater than one log

higher than those observed in normal donors or the subjects themselves at baseline. Thus, rhIL-7 therapy leads to transient, widespread T cell cycling that is tightly regulated by IL-7R α expression, as well as a more sustained increase in bcl-2 expression, resulting in dramatic increases in T cell numbers persisting for several weeks after cessation of therapy. These rhIL-7-expanded T cells retain robust proliferative capacity, even to low level of TCR triggering, a finding that is consistent with IL-7's known capacity to costimulate TCR signaling and to mediate augmented responses to weak antigens (21).

Effects of IL-7 versus IL-2 administration in selected T cell subpopulations

rhIL-2, the only γc cytokine routinely administered therapeutically to humans, also increases CD4 $^+$ T cell numbers in vivo (34, 35). However, IL-2-induced expansion of CD4 $^+$ T cell populations in humans involve selective expansion of CD4 $^+$ CD25 hi , FOXP3 $^+$ T reg cells (34–36), as predicted by the CD25 expression that is the hallmark of this subset. Low level IL-7R α expression on T reg cells (26, 27) suggests that IL-7 therapy may not selectively expand this subset. To assess whether CD4 $^+$ expansion was associated with preferential T reg cell expansion, FOXP3 mRNA was quantified in sorted CD4 $^+$ T cells before and after rhIL-7 therapy (Fig. 3 B). FOXP3 mRNA was not increased in CD4 $^+$ cells collected during the period of CD4 $^+$ expansion, nor was any significant FOXP3 mRNA detected in CD8 $^+$ cells at baseline or after therapy. These mRNA data are corroborated by multicolor flow cytometry analyses performed in selected patients from cohort 4, specifically addressing rhIL-7-induced proliferation in FOXP3 $^+$ and FOXP3 $^-$ subsets. In summary, after 1 wk of treatment with rhIL-7, there is a mean 4.3-fold increase of the percentage of CD4 $^+$ /FoxP3 $^+$ /Ki67 $^+$ cells, whereas the mean fold increases for CD4 $^+$ /FoxP3 $^-$ /Ki67 $^+$ cells and for CD8 $^+$ /FoxP3 $^-$ /Ki67 $^+$ cells are 53.4- and 63.9-fold, respectively. After 2 wk of treatment, the mean fold increases are 1.6-, 24.1-, and 35.7-fold, respectively, whereas at week 3, 1 wk after the end of treatment, they are 0.2-, 5.9-, and 9.6-fold. Representative two-dimensional plots and overlay histograms in one patient are shown in Fig. 3 C.

Thus, in contrast to rhIL-2, rhIL-7 therapy in humans induces robust CD4 $^+$ T cell expansion without selective expansion of T reg cells, which is consistent with a recent study from a separate cohort of subjects in another clinical trial of rhIL-7 (28). Furthermore, multiple studies have also demonstrated that in vivo IL-2 administration in humans has minimal effects on CD8 $^+$ T cells numbers (37, 38). In contrast, we show that the in vivo effects of rhIL-7 on the expansion of CD8 $^+$ T cells are, at a minimum, comparable if not superior to the effects on CD4 $^+$ T cells.

rhIL-7 increases TCR repertoire diversity

Because rhIL-7 receptor expression is high on resting, naive populations, we postulated that the rhIL-7-induced increase in circulating T cells could preferentially expand naive cells,

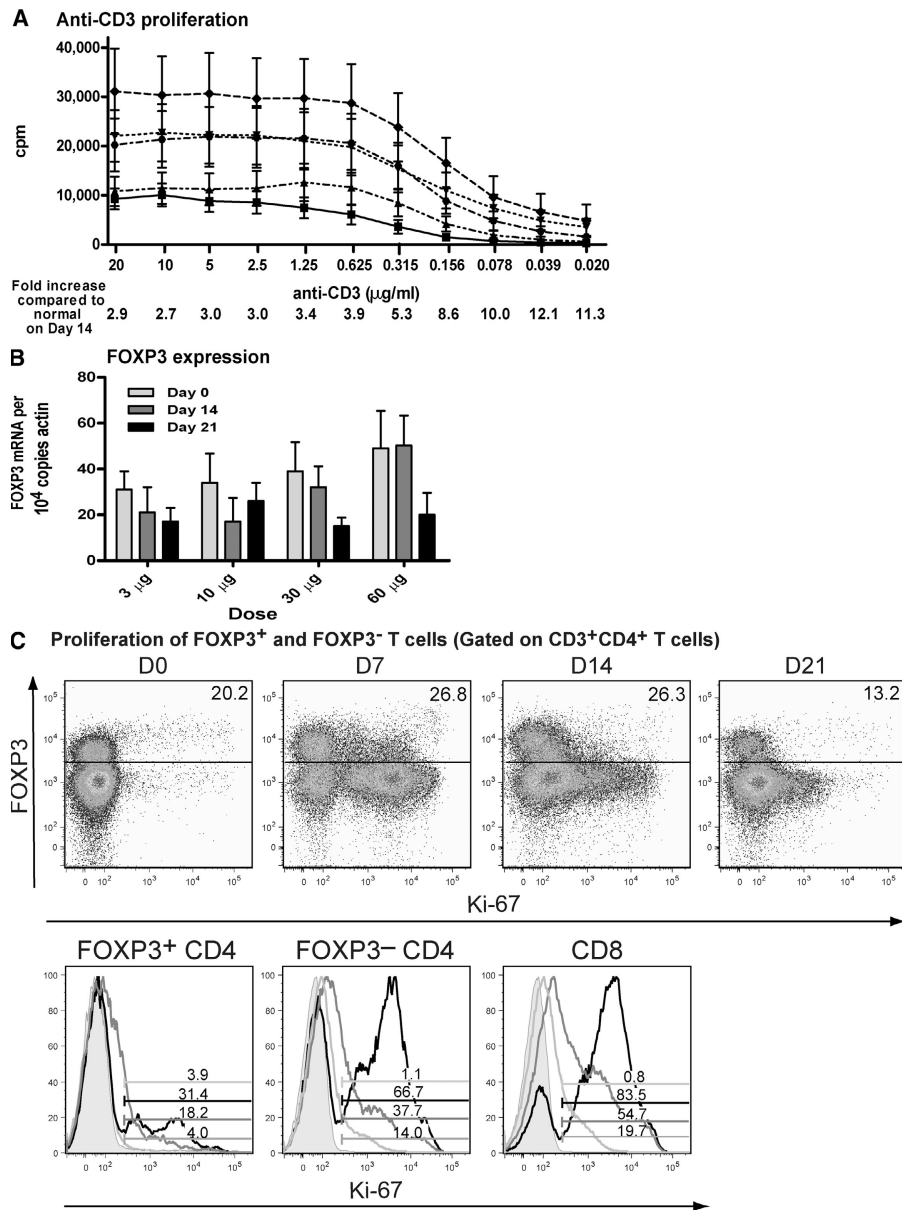


Figure 3. rhIL-7-expanded T cells show robust proliferative responses to CD3 signaling and are not enriched for FOXP3 expressing cells.

(A) PBMCs were collected at the time points shown, cryopreserved, and then thawed before analysis. Proliferation in response to titrated doses of plate-bound anti-CD3 was measured by ^{3}H incorporation, as described in the Materials and methods. Similar increases in CD3-induced proliferation were observed across dose levels, therefore results for all dose levels are pooled ($n = 15$) and compared with normal donors run simultaneously (solid line with □, $n = 16$). rhIL-7-treated subjects showed increased proliferative responses to anti-CD3 on day 7 (dotted line with ▽), day 14 (dashed line with ◆), and day 21 (dashed line with ●) compared with normal donors and on day 7 and 14 compared with baseline values (dashed and dotted line with filled ▲; $P < 0.05$, two-tailed Mann-Whitney test). (B) FOXP3 mRNA copies per 10^4 AXTB mRNA were quantified from sorted CD3⁺/CD4⁺ cells as detailed in the Materials and methods. No significant change in FOXP3 mRNA was detected between baseline values (white) and values obtained at the time of CD4⁺ expansion (day 14 in gray and day 21 in black; $P = \text{NS}$). Mean \pm the SEM of data from subjects enrolled at each dose level are shown: 3 $\mu\text{g/kg}$ ($n = 2$), 10 $\mu\text{g/kg}$ ($n = 3$), 30 $\mu\text{g/kg}$ ($n = 4$), and 60 $\mu\text{g/kg}$ ($n = 5$). (C) Two-dimensional plots (top) and overlay histograms (bottom) of Ki67 expression in T reg cells and other CD4⁺ and CD8⁺ T cells in an individual subject. Percent Ki-67⁺ cells are indicated in each frame. Pretreatment, shaded histograms; day 7, black; day 14, dark gray; day 21, light gray.

and therefore lead to an overall increase in TCR diversity. TCR diversity spectratype analysis was performed on sorted CD4⁺ and CD8⁺ populations before and after (day 21) rhIL-7 therapy in 6 subjects treated at either 30 or 60 $\mu\text{g/kg}$, and

the pre- and post-therapy spectratype divergence from a normal donor standard was assessed (see Materials and methods). Indeed, 4 of the 6 subjects tested had a statistically significant increase in repertoire diversity by 1 wk after the end of treatment

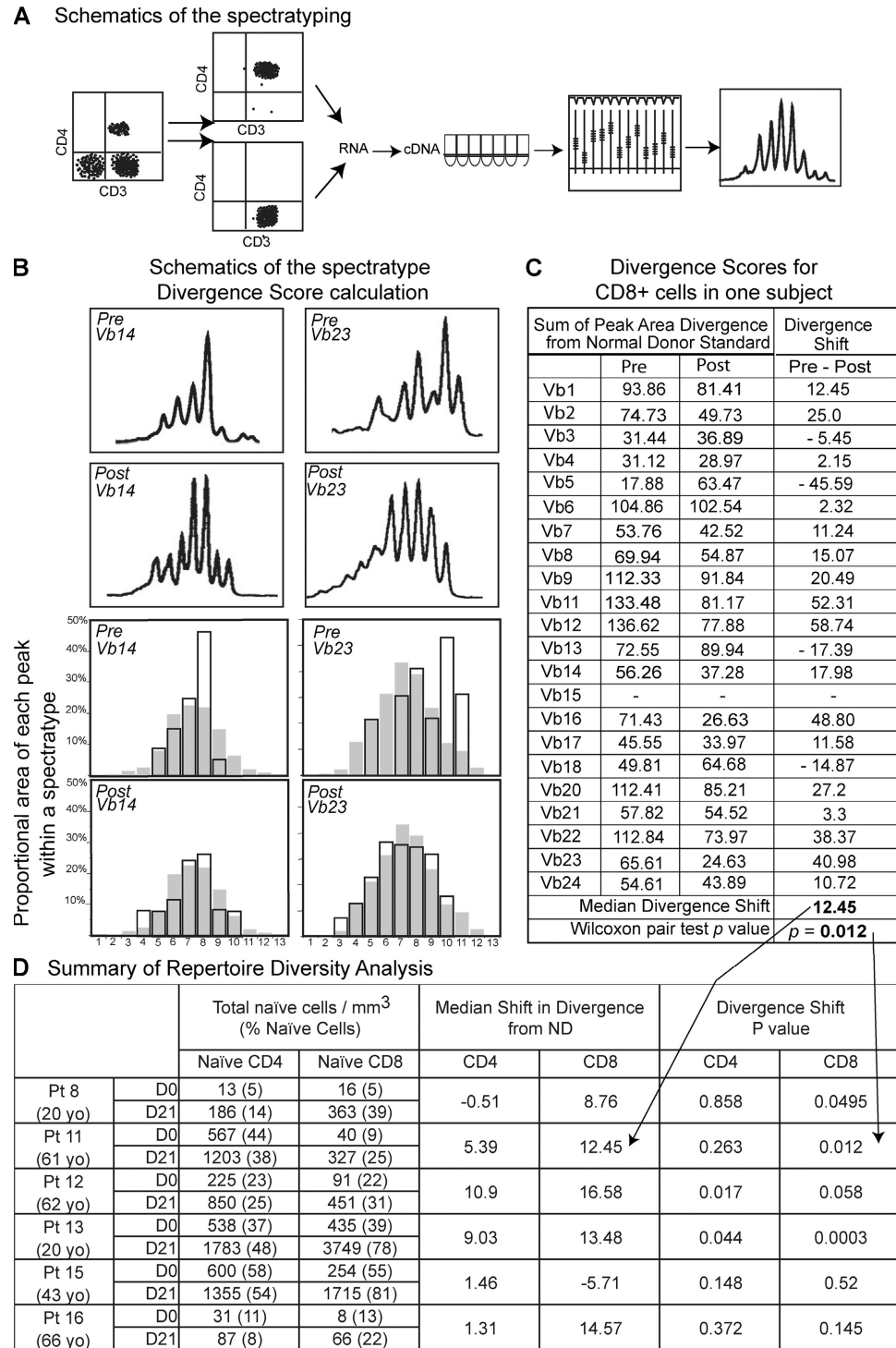


Figure 4. rhIL-7 therapy increases TCR repertoire diversity by Vβ family spectratyping analysis. (A) Schematic representation of the methodology. Vβ family spectratyping analysis was performed for each of 6 subjects (3 of each cohort 3 and 4), separately on CD4+ and CD8+ cells by RT-PCR on RNA extracted from sorted T cells at baseline and at D21. The distributions of peaks for each Vβ family are graphically represented on a curve. (B) Schematic of divergence score calculation. Divergence from the normal donor standard was calculated for each Vβ family, separately for CD4+ and CD8+ cells, for each individual, at baseline and at day 21. Two Vβ families (Vβ14 on the left and Vβ23 on the right) are illustrated for the sorted CD8+ population in one individual (Pt 11), pre (rows 1 and 3), and post (rows 2 and 4) therapy. Overlays of histograms for the subject (no color) and the normal donor standard (in gray) illustrate how the divergence scores were calculated (see Materials and methods). (C) Divergence scores for CD8+ cells in one subject. Divergence scores are shown at baseline (pre) and day 21 (post) for each Vβ family, and a diversity shift was obtained (Pre-Post). The median diversity shift (a positive value indicates a shift toward greater repertoire diversity) and the P value of Wilcoxon pair test comparing the pre and post divergence scores are shown.

(day 21) compared with baseline in CD4⁺, CD8⁺, or both T cell populations (Fig. 4). The two other subjects showed a strong trend in at least one population. Such changes are surprising given the short time period that had elapsed since beginning rhIL-7 therapy, as eliciting spectratype profile differences would be difficult both in the case of individuals with an initially very diverse repertoire (hence, with little possibility of improvement) and of those with a severely depleted repertoire (with marked divergence from a normal donor standard).

rhIL-7 therapy selectively expands CD4⁺ recent thymic emigrants (RTEs), naive cells, and central memory populations, but not effector T cells

IL-7R α expression is tightly regulated during postthymic T cell differentiation, such that RTEs (25, 39), naive, and early memory populations (40) express high IL-7R α levels, whereas effectors and late memory/senescent populations express lower levels (41, 42). To determine whether the effects of rhIL-7 therapy on TCR repertoire diversity could be explained by varied effects among peripheral T cell subsets with differential IL-7R α expression, we measured cycling rates, bcl-2 expression, peripheral blood frequencies, and absolute numbers of RTEs, naive, effector, and memory populations before, during, and after therapy. Fig. 5 illustrates representative changes in a single subject (treated at 60 μ g/kg), Fig. 6 summarizes findings across subjects and dose levels; detailed kinetics for all subsets are included in Fig. S2 (available at <http://www.jem.org/cgi/content/full/jem.20071681/DC1>). Using CD45RA with CD27 or CCR7 coexpression to define the naive subsets, rhIL-7 therapy preferentially expanded naive CD4⁺ and CD8⁺ T cells, leading to increased frequency (Fig. 5, A and C) and absolute numbers (Fig. 6, A and D). Similarly, CD4⁺ RTEs defined by coexpression of CD45RA and CD31 substantially increased both in frequency and number after rhIL-7 therapy. In addition, modest expansion of the memory and effector subsets were observed (Fig. 6 A), which appeared to preferentially involve CD4⁺ central memory cells (Fig. 6 D). Of all subsets, the naive CD8⁺ expanded the most and significantly more than the CD8⁺ memory and effector subsets ($P = 0.008$), and these effects were similar regardless of subject age (Fig. S1 B). This preferential effect on naive cells, including RTEs, was not caused by differences in maximal Ki67 expression because rhIL-7 similarly increased the cycling rate of nearly all subsets in a steep dose-dependent manner (Fig. 5 B and Fig. 6 B) by day 7 of therapy, followed by a gradual return to near baseline by day 21 (Fig. 5 B and Fig. S2). Interestingly, however, whereas memory and effector subsets showed a brisk decline in Ki67 frequency by day 14,

there remained a distinct subset of Ki67⁺ cells at this time point in both CD4⁺ and CD8⁺ naive subsets (Fig. 5 B). rhIL-7 also induced a dose-dependent increase in bcl-2 mean fluorescence intensity (MFI) in all subsets except CD8⁺ effectors (Fig. 6 C). Thus, rhIL-7 therapy increased total body T cell mass with preferential expansion of the naive subsets, resulting in a T cell pool in this adult population that more closely resembles that seen earlier in life. This could potentially relate to fine differential kinetics of cell cycling, IL-7R α expression, or bcl-2 up-regulation, although changes in these parameters of similar magnitude were observed in nonnaive subsets as well (Fig. S2). Alternatively, these results could suggest that, after similar levels of rhIL-7 signaling, naive T cells undergo a greater proliferative burst than memory or effector subsets and/or that some component of the increase in naive subsets reflects input of cells from an alternative source.

rhIL-7 increases circulating TCR excision circles (TRECs) numbers

Because rhIL-7 preferentially increases RTEs and naive T cells, we investigated a potential thymic contribution to its effects. Peripheral blood TREC⁺s have been used as an indirect measure of thymic output because they reflect TCR gene recombination events and are enriched within the RTE fraction (43). Because TREC⁺s are nonreplicating DNA, however, they become diluted with T cell division and, in preclinical primate studies (19, 20), TREC frequencies diminished after rhIL-7 therapy, presumably caused by induced cycling in RTEs (44). In this study, we observed diminished absolute numbers of circulating TREC⁺s/milliliter on day 7 (Fig. 7 A), an expected reflection of the diminished total number of circulating phenotypically naive cells at that point, followed by an increase in the absolute number of TREC⁺s/mm³ (doubling in the 2 highest dose cohorts) between days 7 and 21, which is consistent with the subsequent rise in naive T cell absolute number. Despite widespread rhIL-7-induced T cell cycling, TREC⁺ frequencies were largely unchanged in sorted CD4⁺ and CD8⁺ peripheral T cells before and after therapy (Fig. 7 B). The absence of profound reductions in TREC frequencies in the face of significant T cell cycling raises the possibility that rhIL-7 might also induce new thymic emigrants to enter the circulation. However, in other clinical settings such as after chemotherapy, where a substantial thymic output increase does occur, it occurs later, is preceded by a thymic size increase on CT scan, is accompanied by a >10-fold increase in TREC, and the magnitude of the effects diminishes with increasing age (30, 45). We observed no increase in thymic size on day 14 or 28 CT scans after rhIL-7 therapy, and there was not a significant correlation

and then incorporated into the summary in D. (D) Summary of repertoire diversity analysis. for each tested individual (age), shown at baseline (D0) and D21 are as follows: the total naive CD4⁺ and naive CD8⁺ cells counts; the median diversity shift for each CD4 and CD8 subsets of each individual and the P values of the Wilcoxon pair test indicating the likelihood that the calculated change in divergence scores for a particular subject's CD4⁺ or CD8⁺ cells between day 21 and baseline occurred by chance; P values <0.05 indicate a statistically significant increase in diversity toward normality between baseline and day 21 studies.

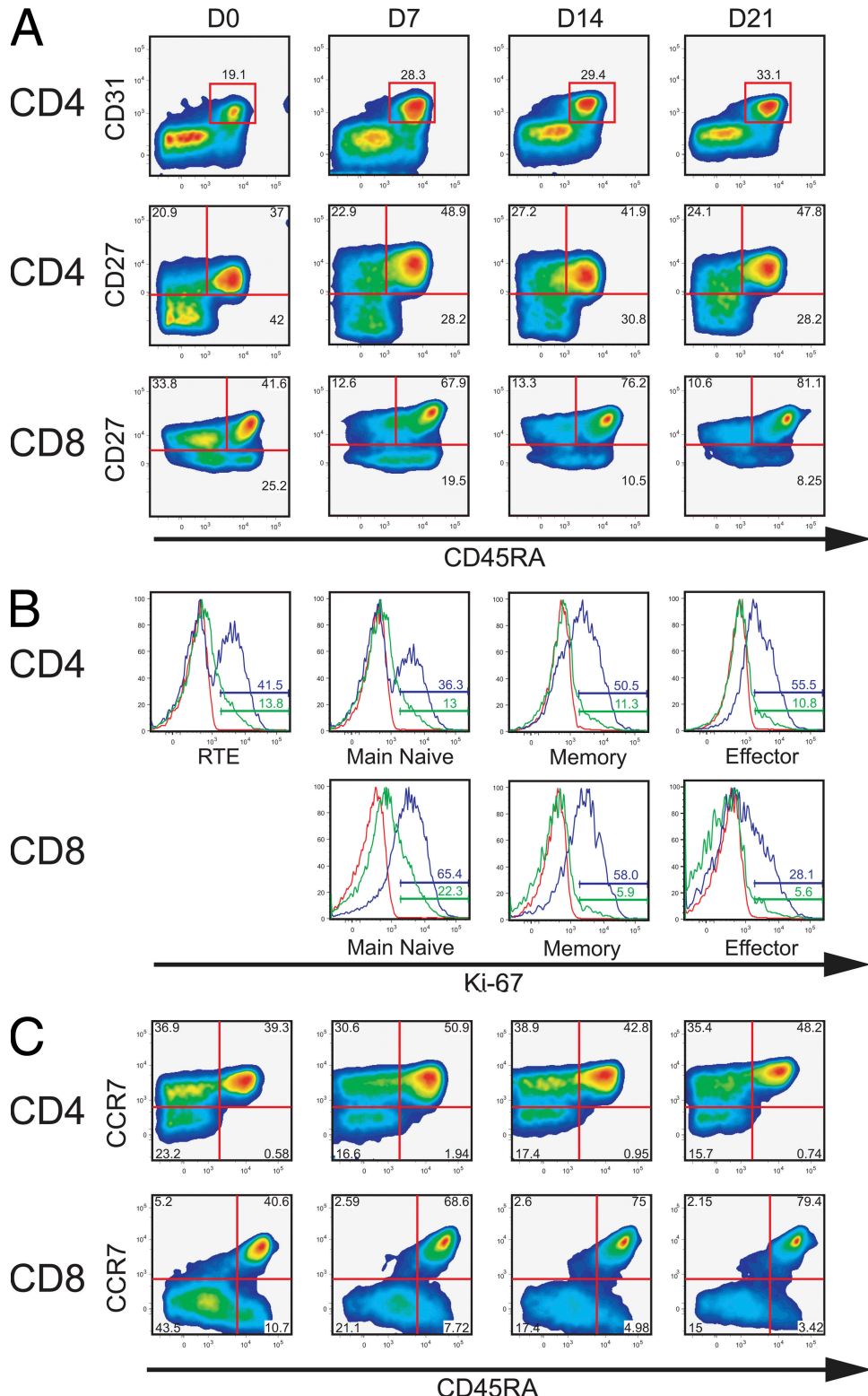


Figure 5. rhIL-7 therapy induces cycling of most T cell subsets, but preferentially expands naive CD4⁺ and CD8⁺ cells and CD4⁺ central memory cells. Representative data from a single subject treated at 60 µg/kg/d are shown. (A) Two-dimensional plots illustrating the rhIL-7 therapy-induced increased frequency of CD4⁺ RTEs (CD31⁺/CD45RA⁺; red boxes in first row of graphs), and changes in CD4⁺ and CD8⁺ naive, memory, and effector subsets (respectively CD45RA⁺/CD27⁺, CD45RA⁻/CD27⁺, and CD45RA⁻/CD27⁻ sections on second and third rows). (B) Overlay histograms of Ki-67 expression on CD4⁺ RTEs (CD31⁺/CD45RA⁺) and CD4⁺ and CD8⁺ naive (CD45RA⁺/CD27⁺), memory (CD45RA⁻/CD27⁺), and effector (CD45RA⁻/CD27⁻) subsets. Percent Ki-67⁺ cells are indicated in each frame. Red lines, pretreatment; blue lines, day 7; green lines, day 14; orange lines, day 21. Note that at

between age and TREC increase (Fig. S1 B). We also performed a similar TREC analysis on sorted naive CD4⁺/CD31⁺/CD45RA⁺ cells and naive CD8⁺/CD27⁺/CD45RA⁺ cells before and after rhIL-7 therapy to probe for increased cycling of this subset resulting in TREC dilution. Indeed, in the two individuals studied, we observed pronounced dilution of TRECs (reduction by 80 and 62% of TRECs/200K RNaseP copies in sorted CD4⁺ RTEs, and reduction by 32 and 56% of TRECs/200K RNaseP copies in sorted CD8⁺ naive T cells) after rhIL-7 therapy, which is consistent with intense proliferation in these subsets. Therefore, although rhIL-7–induced augmentation of thymopoiesis cannot be ruled out, the available data are most consistent with rhIL-7–induced entry of new thymic emigrants into the circulation via mobilization from lymphoid sites and/or enhanced thymic egress, as previously observed in an animal model of IL-7 administration (25), in concert with vigorous cycling of the naive and RTE subsets.

In summary, rhIL-7 induces increases in total body T cell mass accompanied by an age-independent overall increase in TCR repertoire diversity. Preferential expansion of naive subsets leads to an increased TCR diversity and changes in peripheral T cell subset compositions that reverse the aged phenotype. The timing of this increase, the lack of frank increase in the absolute number of circulating TRECs, the marked dilution effect on TRECs in the naive subsets of selected individuals, and the detailed phenotypic analysis of T cells subset kinetics indicate that this increase in TCR diversity primarily arises from the preferential peripheral expansion of the RTEs and naive T cells, the most diverse components of the T cell pool.

DISCUSSION

Administration of supraphysiologic doses of recombinant growth factors to augment hematopoietic cell recovery has had a substantial impact in medical practice, with recombinant proteins now available to enhance red cell, white cell, and platelet regeneration approved for clinical use. Thus far, however, no agent able to safely expand a broad repertoire of T cells has been identified, and impaired immune reconstitution remains problematic in many clinical settings (46). Several preclinical studies have implicated IL-7 as a primary modulator of peripheral T cell homeostasis with potent immunorestorative properties, raising the prospect that rhIL-7 may serve as a clinically effective T cell growth factor. This study demonstrates that rhIL-7 administration in humans can safely induce polyclonal T cell expansion *in vivo*, resulting in dramatic increases in T cell number. Although the clinical details associated with the therapy are the focus of a separate report (unpublished data), the agent was well tolerated on this trial. Mechanistically, the effect of rhIL-7 can be attributed to a

combination of increased cell cycling, likely via TCR triggering to cross-reactive self-antigens, and diminished programmed cell death, which was self-limited by down-regulation of IL-7R α in the face of continued drug administration. The rhIL-7–expanded T cells remained functional, retaining robust responsiveness to TCR triggering with even a suggestion of increased sensitivity to TCR ligation after a suboptimal stimulus, as seen in preclinical models.

rhIL-7 preferentially expanded naive CD4⁺ and CD8⁺ subsets, including the most naive circulating RTEs (CD4⁺/CD45RA⁺/CD31⁺), consistent with the results from mouse studies (44). The effects on CD4⁺ and CD8⁺ memory cells and CD4⁺ effectors were intermediate, whereas CD8⁺ effectors underwent little expansion. Notably, rhIL-7–expanded central memory CD4⁺ T cells, a subset that may be critically important in avoiding clonal exhaustion in the context of chronic persistent viral or tumoral antigenic exposure (47, 48). It is also noteworthy that rhIL-7 preferentially expanded the two subsets of T cells capable of initiating lymph node germinal center formation, the naive and central memory subsets.

Despite the clear evidence presented in this study that rhIL-7 therapy substantially increases TCR diversity by an increase in the size of the naive T cell pool, the contribution of the thymus to these rapid changes remains unclear. Pre-clinical studies provide evidence both for and against rhIL-7–induced augmentation of thymopoiesis (18–20). In this study, we observed increases in absolute numbers of TRECs (albeit modest) and in numbers of peripheral blood phenotypic RTEs. However, we saw neither evidence for thymic enlargement nor significant correlation between age and rhIL-7 effects. Furthermore, our TREC analysis on sorted naive CD4⁺/CD31⁺/CD45RA⁺ cells and naive CD8⁺/CD27⁺/CD45RA⁺ cells shows a pronounced dilution effect of TRECs consistent with the intense proliferation in these subsets, thus arguing that the observed effect on repertoire diversity is in large part caused by decreased skewing by proliferation of RTEs. Together, these data suggest that the observed changes reflected rhIL-7–induced increases in RTE cycling, as well as trafficking of RTEs from peripheral lymphoid tissue into the bloodstream as seen in the mouse model (25, 44), whereas no direct effect on thymopoiesis can be demonstrated in the short time span of this study. Indeed, in clinical settings, thymic participation in immune reconstitution in adults is delayed for several months after the depleting event (30), raising the possibility that more direct thymopoietic effects of rhIL-7, if induced, could require more chronic rhIL-7 administration. However, even if the observed rhIL-7 effects are thymic independent and reflect naive cell expansion rather than increased thymic throughput per se, the net effect of rhIL-7 therapy remains a substantial, measured, increase in

the end of treatment (green line), the percentage of Ki67⁺ memory and effector CD8⁺ populations drop to lower levels than the naive CD8⁺. (C) Two-dimensional plots illustrating the rhIL-7 therapy-induced changes in CD4⁺ (top row) and CD8⁺ (bottom row) naive, central memory, effector memory, and effectors (respectively CD45RA⁺/CCR7⁺, CD45RA⁻/CCR7⁺, CD45RA⁻/CCR7⁻, and CD45RA^{+/}-CCR7⁻ sections).

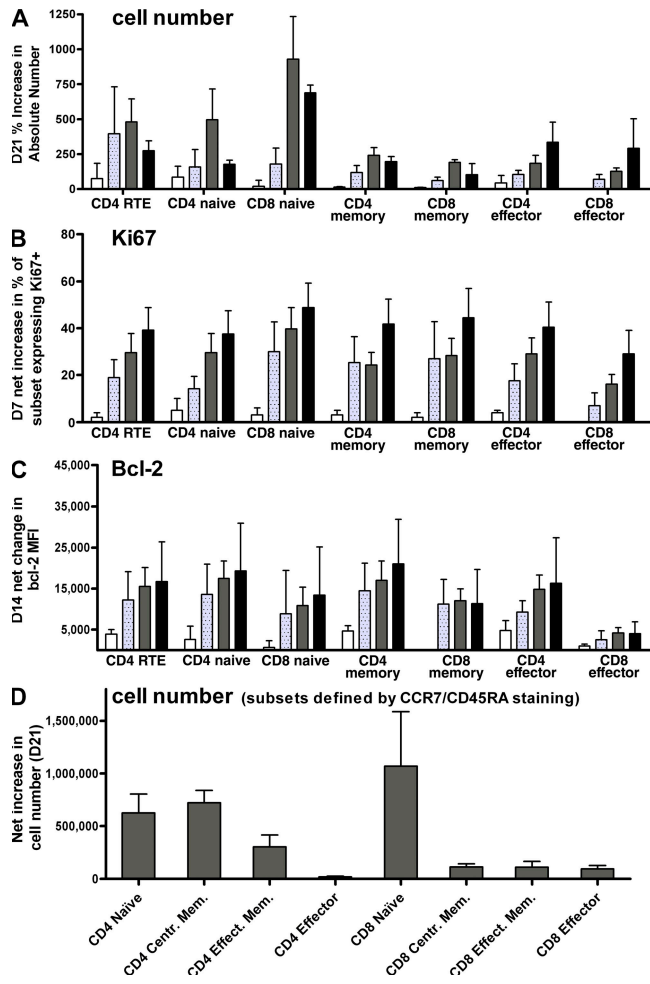


Figure 6. rhIL-7 induces cycling and increases bcl-2 expression across subsets, but preferentially expands naive T cells and CD4⁺ memory cells. Changes in cell number (A), Ki-67 expression (B), and bcl-2 expression (C) are shown for subjects treated at 3 µg/kg/d (white), 10 µg/kg/d (speckled), 30 µg/kg/d (gray), and 60 µg/kg/d (black). The time points shown represent the point of maximal increase for each parameter, as illustrated in Fig. 1, as follows: day 21 for increase in cell number, day 7 for Ki-67, and day 14 for bcl-2 expression. (A) Percent increase in absolute circulating cell number (per milliliter) over pretherapy value for each subset at day 21 after rhIL-7. Percent increase in the naive CD8⁺ subset were significantly higher than for the CD8⁺ memory ($P = 0.008$) or CD8⁺ effector subsets ($P = 0.008$). (B) Net increase in the proportion of Ki67⁺ cells in each subset at day 7 was calculated by subtracting the percentage of each subset that expressed Ki-67 at baseline from the percentage expressing Ki-67 at day 7 of rhIL-7 therapy. (C) Net increase in bcl-2 MFI in each subset at day 14 was calculated by subtracting the MFI of bcl-2 expression at baseline from the MFI on day 14 after rhIL-7 for each subset. See Fig. S2 for detailed data on changes in subset parameters for each dose level. (D) Net increase in cell number at day 21 in subsets defined by CCR7 and CD45RA surface expression (see Materials and methods) as follows: naive (CCR7⁺CD45RA⁺), central memory (CCR7⁺CD45RA⁻), effector memory (CCR7⁻CD45RA⁻), and effector RA (CCR7⁻CD45RA⁺). Mean value for the six studied subjects. Error bars represent the SEM. Fig S2 is available at <http://www.jem.org/cgi/content/full/jem.20071681/DC1>.

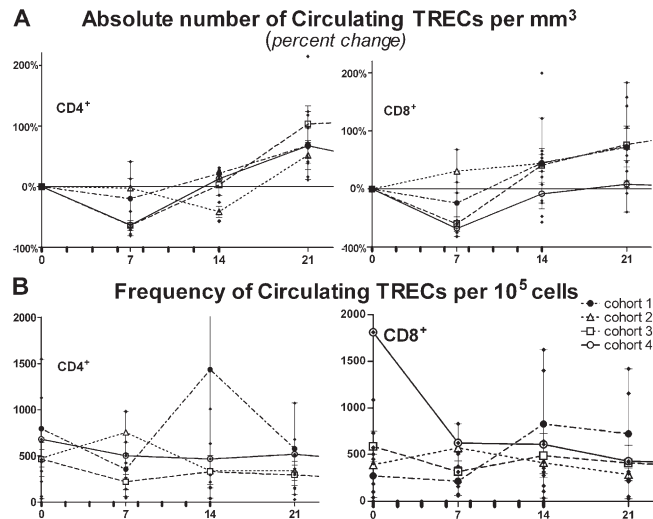


Figure 7. rhIL-7 therapy increases the number of TREC-expressing cells in the peripheral blood. We measured TREC in sorted CD4⁺ and CD8⁺ T cells at the time points shown, and values shown were normalized per 10⁵ cells. Individual subjects (●); mean of cohort (± the SEM): 3 µg/kg/d (dashed line with ●), 10 µg/kg/d (dotted line with △), 30 µg/kg/d (dashed line with □), 60 µg/kg/d (solid line with ○). Tick marks represent rhIL-7 injections. (A) Absolute number of circulating TREC/mm³ of blood diminished during the first 7 d of rhIL-7 therapy, consistent with a decrease in naive populations during this period. Rises in TREC were observed from day 7–28, consistent with increased numbers of enumerated phenotypically naive cells during this period. (B) No significant changes in the frequency of TREC/10⁵ sorted total CD4⁺ or CD8⁺ cells was observed, despite increases in cell cycling shown in Figs. 1 and 6 (see text for TREC in naive subsets).

TCR repertoire diversity in adult subjects, thereby reshaping their T cell pool. During the aging process, the accumulation of senescent and more oligoclonal CD8⁺ cells with a terminal differentiation phenotype has been associated with dysfunctional immune responses (49). The effects of rhIL-7 on naive and central memory subsets could restore balance in T cell subsets during immunological aging and restore a T cell profile resembling that seen earlier in life. Such “antiaging” effects could prove beneficial for T cell-depleted hosts or older hosts, where the combined loss of total T cell number, naive cells, and the corollary loss of repertoire diversity appears to contribute to diminished overall immune responsiveness.

In summary, in this first clinical trial of rhIL-7 initiated in humans, and after the brief study of another National Cancer Institute-initiated trial (28), we present evidence that rhIL-7 therapy in humans induces dramatic, polyclonal, prolonged CD4⁺ and CD8⁺ T cell expansion in vivo, with preferential increases in T cells bearing diverse TCR repertoire specificities. The effects are mediated primarily through increased peripheral T cell cycling and augmented cell survival. The rhIL-7-expanded T cells retain significant functional capacity, and the CD4⁺ T cell expansion is not accompanied by a disproportional increase in T reg cells, such as that which occurs after rhIL-2 therapy. rhIL-7 appears to be an effective T cell growth factor

with “immune rejuvenating” properties that suggest it would be effective in augmenting immune reactivity in hosts with impaired immunity caused by physiological (age), iatrogenic (chemotherapy/transplantation), or pathological (HIV) lymphodepletion. In immunologically normal, as well as deficient hosts, rhIL-7’s capacity to augment responses to weak antigens and to increase T cell cycling without T reg cell expansion may be clinically exploitable in the context of immunotherapy regimens for cancer and/or chronic infection. Future clinical studies of rhIL-7 in the context of immune-based therapies are warranted.

MATERIALS AND METHODS

Subject population and trial design

We enrolled 16 subjects with nonhematologic, nonlymphoid cancer refractory to standard therapy on a standard phase I dose escalation study of rhIL-7 (National Cancer Institute, NCI protocol 03-C-0152). The study was approved by the Institutional Review Board of the NCI and by the Food and Drug Administration. All subjects signed a written informed consent before enrollment. Subjects received subcutaneous injections of rhIL-7 (provided by Cytheris Inc., Rockville, MD) at the doses noted every other day for eight doses. A maximum tolerated dose was not reached on this study, and two subjects experienced dose limiting toxicity. One patient treated at 30 µg/kg/d received only one injection before being removed from the study (because of a grade 3 transaminase elevation) and is not included in the analyses. Another subject was removed from study (because of grade 3 hypertension and chest pain) after receiving the first four injections at 60 µg/kg/d and is included in the relevant analyses. Significant differences in the pattern of total lymphocyte expansion were not seen when this subject was compared with the study subjects who completed the treatment. A detailed description of the eligibility criteria, subject population, and clinical results of this trial is the object of a separate report (unpublished data).

Flow cytometry and cell sorting

PBMC analysis. We used flow cytometry to assess the intracellular and cell surface expression of selected markers on PBMCs at the specified time points. We analyzed EDTA anticoagulated peripheral blood specimens on the same day without cryopreservation; the specimens were handled according to established clinical guidelines. We stained 3 ml of the samples for 4-color flow cytometry using a whole-blood lysis method; the samples were analyzed on a FACSCalibur (BD Biosciences) using CellQuest software (BD Biosciences). We used an additional 5 ml of blood to generate mononuclear cells via density gradient separation for determination of intracellular Ki-67 expression in T cells and T cell subsets. We identified T cells and T cell subsets using directly conjugated monoclonal antibodies: anti-CD3, -CD4, -CD8, - α/β TCR, and - γ/δ TCR; T cells were further characterized using anti-CD9, -CD11a, -CD71, -CD127, -CD184, and -Ki-67. We evaluated B cells with anti-CD20 and NK cells with a combination of anti-CD16 and -CD56, evaluated on CD3+ lymphocytes. We used directly conjugated, mouse IgG1 to ascertain background staining. We identified lymphocytes based on a gate established by forward and side-angle scatter, and confirmed using anti-CD45/-CD14 (Leukogate; BD Biosciences). The absolute number for each population was generated using absolute peripheral blood lymphocyte count, determined by a Cell Dyn Sapphire (Abbott). We used peripheral blood from healthy adult controls to establish 95% confidence intervals. We obtained all monoclonal antibodies from BD Biosciences, with the exception of anti-CD4, -CD8, -CD127, and - α/β TCR (Beckman Coulter), anti- γ/δ TCR (Pierce-Endogen), and anti-CD11a (Dako).

CD4+ and CD8+ T cell subset analysis

We further analyzed cryopreserved PBMC to examine T cell subsets, markers of cell proliferation and apoptotic susceptibility within these subpopulations.

We stained cells with CD8-Pacific Blue, CD3-APC-Cy5.5, CD45RA-PECy5 (all Invitrogen), CD27-APC (eBioscience), CD4-APC-Cy7, and CD31-FITC (all BD Biosciences); fixed; permeabilized (BD Biosciences); stained for intracellular markers with isotype control-PE, Ki-67-PE or Bcl-2-PE (all BD Biosciences); and analyzed on a LSR II flow cytometer (BD Biosciences) equipped with violet 405, argon 488, and HeNe 635 lasers. We acquired data using DIVA software (BD Biosciences) and analyzed using FlowJo (Tree Star, Inc.). Gating on populations of CD3+CD8+ and CD3+CD4+ T cells, expression of Ki67 or bcl-2 was determined on T cell subsets defined by the following antibody expression patterns: RTEs as CD4+/CD45RA+/CD31+, naive CD4 or CD8 T cells as CD27+ CD45RA+, memory as CD27+CD45RA-, and effector T cells as CD27- CD45RA+-. Alternatively, cells were stained with CCR7-FITC (R&D Systems), and the remaining surface markers and analyzed for naive (CCR7+CD45RA+), central memory (CCR7+CD45RA-), effector memory (CCR7-CD45RA-), and effector RA (CCR7-CD45RA+), following the research of Sallusto et al. (50). We calculated the absolute cells number/mliter expressing a particular phenotype by multiplying the frequency of the subset within CD4 or CD8 T cells by the absolute number of those cells as calculated during cytometric analysis of fresh whole blood.

IL-7RA, FOXP3 message determination

We used electronically sorted CD4+ and CD8+ populations for RNA extraction. We extracted RNA using Trizol (Invitrogen) according to the manufacturer’s instructions, and then reverse transcribed 500 ng of RNA using the SuperScript III First-Strand Synthesis System (Invitrogen). We performed quantitative PCR using the Taqman ABI Prism 7000 Sequence Detection System (Applied Biosystems) on cDNA samples for FOXP3 and IL-7RA expression, and normalized them to the housekeeping gene ACTB. We purchased probes for detection of FOXP3, IL-7RA, ACTB, and the Taqman Universal PCR Master Mix (Applied Biosystems) and used them according to the provided protocol. We generated standard curves to quantify FOXP3, IL-7RA, and ACTB by cloning FOXP3, IL-7RA, and ACTB PCR products into plasmids using Platinum Taq and TOPO TA Cloning kit (Invitrogen) as per the manufacturer’s instructions. PCR conditions were a 94°C 2-min hot start followed by 94°C for 30 s, 58°C for 30 s, 72°C for 45 s for 30 cycles, and culminating in a final 72°C 7-min extension step. Primer sequences were as follows: ACTB, 5'-GAGCACAGAGCC-TCGCCTTG-3' (sense), 5'-CGCCCACATAGGAATCCTTCT-3' (antisense); FOXP3, 5'-GCACCTCCCAAATCCCAGT-3' (sense), 5'-GCAGGCAAGACAGTGGAAACC-3' (antisense); IL-7RA proprietary (“HS00233682” from ABI).

T cell proliferation in response to anti-CD3 signaling

We thawed PBMC cryopreserved at each time point, and then incubated it for 2 d in 200 µl/well of 10% human AB serum/ AIM-V medium on 96-well flat-bottomed plates (Nunc) coated with the designed concentrations of OKT3 (Orthoclone). We measured cell proliferation by incorporation of [³H]thymidine (1 µCi/well; ICN) after a 16–18-h pulse. Cpm reflects proliferation after anti-CD3 minus cell proliferation in the medium. We ran normal donor controls with each assay.

TREC analysis

For TREC analysis, we sorted CD3+CD4+ and CD3+CD8+ T cells and, in two subjects, CD4+/CD31+ and CD8+/CD45RA+ T cells from cryopreserved PBMC on a FACS Vantage (D Biosciences). Real-time quantitative-PCR was performed using the 5'-nuclease (Taqman) assay on cell lysates on an ABI7700 system (Applied Biosystems) according to the protocol of Douek et al. (43). Cells were lysed in 100 µg/ml proteinase K (Boehringer-Mannheim) in 10 mM TRIS, and heated for 1 h at 56°C, and then for 10 min at 95°C. PCR reactions contained Platinum Quantitative PCR SuperMix-UDG with ROX (Invitrogen) with 500 nM of each primer, and 150 nM probe. PCR conditions were 95°C for 5 min, 95°C for 30 s, and 60°C for 1 min for 40 cycles. The forward and reverse TREC primers were 5'-CACATCCCTTCAACCAT-GCT-3' and 5'-GCCAGCTGCAGGGTTAGTG-3', respectively, and

the probe FAM-5'-ACACCTCTGGTTTGTAAAGGTGCCCACT-TAMRA (Integrated DNA Technologies, Inc.). A standard curve (10^{2-7} TREC copies/well) was plotted using a plasmid containing the TREC gene sequence (provided by D.C. Douek, National Institutes of Health, Bethesda, MD). We normalized TREC values to cell content by concurrent measurement of the single-copy gene, RNase P, using the TaqMan RNase P Control Reagents kit (Applied Biosystems). Samples were analyzed in duplicate, and the results were averaged and normalized as TRECs/200,000 copies RNaseP, equaling TRECs/100,000 cells.

T cell repertoire diversity evaluation and statistical evaluation of TCR β -chain variable region (V β) spectratypes

We performed spectratype analyses separately on CD4 $^+$ and CD8 $^+$ T cell subsets from 6 subjects (3 each of cohorts 3 and 4). We sorted CD3 $^+$ CD4 $^+$ and CD3 $^+$ CD8 $^+$ T cells to 98% purity from cryopreserved PBMC on a FACS Vantage (BDIS). We used 10^5 cells of each to isolate RNA using Trizol (Invitrogen) in the presence of carrier tRNA and glycogen as carrier, and converted to cDNA using Oligo-dT as a primer for reverse transcription (First Strand cDNA kit; Roche). We amplified cDNA in 22 separate PCR reactions (V β families 1–24, excluding V β 10 and 19), each containing 1 specific human V β subfamily primer coupled with an unlabeled consensus C β region primer, followed by a 10-cycle run-off nested PCR reaction, using a FAM-labeled internal BC primer (Integrated DNA Technologies, Inc.). Labeled run-off reaction C β primer and V β family-specific (forward) primers were as specified in Currier et al. (51), except for V β 5, 13, 15, and 16. These remaining V β primers and the C β primer were as from Puisieux et al. (52). The initial and run-off PCR used 0.75 U cloned PFU DNA polymerase (Stratagene), and PCR settings were hot start with 2 min at 95°C followed by 30 cycles of 95°C for 30 s, 55°C for 45 s, and 72°C for 1 min, followed a final extension at 72°C for 10 min. Run-off reaction product was mixed at 1:9 ratio with loading buffer, consisting of Hi-Di Formamide (Applied Biosystems) containing size standards GeneScan-500 ROX, Red A (Applied Biosystems) mixed at a 1:20 ratio. Reactions were heated for 2 min at 95°C, and products were run on an ABI sequencer 3130XI (Applied Biosciences). Peaks were identified in the final spectratype histogram, and the area underneath was determined using GeneMapper v. 3.7 software (Applied Biosciences).

Using this same methodology, we also analyzed each V β family of 10–15 normal donor T cells (CD4 $^+$ and CD8 $^+$ combined), thereby defining “normal donor standards.” For each donor’s spectratype, we aligned the peaks by nucleotide base pair number, and used the area under each of 13 potential peak locations to calculate a total area under the spectratype curve, and then a proportional area for each peak. We then averaged the proportional areas to establish a normal donor standard spectratype. As expected, as we added more donors to the determination, the mean curves approached a more Gaussian-like distribution.

For each study subject, we then quantified the “divergence score” of each V β family from its counterpart V β normal donor standard as the sum of the absolute value of the divergence in proportional area at each peak. Therefore, divergence scores were established for each V β family, for each patient, separately for CD4 $^+$ and for CD8 $^+$ cells, and for both at baseline (pre) and day 21 (post). We then tested the hypothesis that, for a given CD4 $^+$ or CD8 $^+$ population in a given subject, the day 21 (post) divergence scores were significantly smaller than the baseline (pre) divergence scores in a non-parametric Wilcoxon analysis (2-tailed). A P value <0.05 indicates a statistically significant increase in repertoire diversity toward normality between the baseline and day 21 studies.

Finally, for each single V β family, we calculated a “diversity shift” as the difference between “pre” and “post” divergence scores, and we calculated the median of these diversity shifts (median diversity shift) for the set of 22 V β family of each T cell population (CD4 $^+$ or CD8 $^+$), a positive value indicating a shift toward greater repertoire diversity.

Statistical analyses

Anti-CD3 proliferation. We performed statistical analyses using GraphPad Prism version 4.0a for Macintosh (GraphPad Software). Significant differences

when comparing two groups was determined by two-tailed unpaired nonparametric Mann-Whitney test. P values were considered significant if <0.05.

Correlation with age. We evaluated the statistical significance of the correlation of age with the percent increase of various lymphocyte populations, as well as with TRECs, with a Spearman’s correlation test with a significant 2-tailed P value of <0.05 (GraphPad Prism version 4.0a for Macintosh; GraphPad Software).

Spectratyping analysis. See previous section.

Online supplemental material

Fig. S1 shows time courses of various lymphocyte populations following rhIL-7 therapy. Fig. S2 shows time course on percent change over baseline in circulating cells, Ki67 expression, and Bcl-2 up-regulation for all studied subsets. The online version of this article is available at <http://www.jem.org/cgi/content/full/jem.20071681/DC1>.

The authors would like to thank the subjects who enrolled on this investigational trial and provided consent for research studies and the clinical staff of the National Institutes of Health Clinical Center and of the Experimental Transplantation and Immunology Branch for their excellent care of these subjects. We would also like to thank Drs. Al Singer and Scott Durum for helpful comments and careful reviews of the manuscript.

This research was supported by the Intramural Research Program of the National Institutes of Health, National Cancer Institute (NCI), and Center for Cancer Research and was made possible through a formal collaboration (Cooperative Research and Development Agreement [CRADA] #01649) between the NCI and Cytheris Inc., the investigational new drug holder and manufacturer of rhIL-7, currently developing recombinant human IL-7 for therapeutic use. As per the CRADA between NCI and Cytheris Inc., the NCI investigators designed and conducted all the research experiments and analyses presented in the article independently from Cytheris Inc.

Three co-authors have financial interest in Cytheris capital: M. Morre is the founder and Chief Executive Officer and J. Engels and R. Buffet are employees of Cytheris. All other co-authors have explicitly denied any conflict of interest.

Submitted: 8 August 2007

Accepted: 21 May 2008

REFERENCES

- Blattman, J.N., J.M. Grayson, E.J. Wherry, S.M. Kaech, K.A. Smith, and R. Ahmed. 2003. Therapeutic use of IL-2 to enhance antiviral T cell responses in vivo. *Nat. Med.* 9:540–547.
- Khan, I.A., and L. Casciotti. 1999. IL-15 prolongs the duration of CD8 $^+$ T cell-mediated immunity in mice infected with a vaccine strain of Toxoplasma gondii. *J. Immunol.* 163:4503–4509.
- Berzofsky, J.A., J.D. Ahlers, J. Janik, J. Morris, S. Oh, M. Terabe, and I.M. Belyakov. 2004. Progress on new vaccine strategies against chronic viral infections. *J. Clin. Invest.* 114:450–462.
- Wang, L.X., R. Li, G. Yang, M. Lim, A. O’Hara, Y. Chu, B.A. Fox, N.P. Restifo, W.J. Urba, and H.M. Hu. 2005. Interleukin-7-dependent expansion and persistence of melanoma-specific T cells in lymphodepleted mice lead to tumor regression and editing. *Cancer Res.* 65:10569–10577.
- Zeng, R., R. Spolski, S.E. Finkelstein, S. Oh, P.E. Kovanen, C.S. Hinrichs, C.A. Pise-Masison, M.F. Radonovich, J.N. Brady, N.P. Restifo, et al. 2005. Synergy of IL-21 and IL-15 in regulating CD8 $^+$ T cell expansion and function. *J. Exp. Med.* 201:139–148.
- Klebanoff, C.A., S.E. Finkelstein, D.R. Surman, M.K. Lichtman, L. Gattinoni, M.R. Theoret, N. Grewal, P.J. Spiess, P.A. Antony, D.C. Palmer, et al. 2004. IL-15 enhances the in vivo antitumor activity of tumor-reactive CD8 $^+$ T cells. *Proc. Natl. Acad. Sci. USA.* 101:1969–1974.
- Park, J.H., Q. Yu, B. Erman, J.S. Appelbaum, D. Montoya-Durango, H.L. Grimes, and A. Singer. 2004. Suppression of IL7Ralpha transcription by IL-7 and other prosurvival cytokines: a novel mechanism for maximizing IL-7-dependent T cell survival. *Immunity.* 21:289–302.

8. Grabstein, K.H., T.J. Waldschmidt, F.D. Finkelman, B.W. Hess, A.R. Alpert, N.E. Boiani, A.E. Namen, and P.J. Morrissey. 1993. Inhibition of murine B and T lymphopoiesis in vivo by an anti-interleukin 7 monoclonal antibody. *J. Exp. Med.* 178:257–264.
9. von Freeden-Jeffry, U., P. Vieira, L.A. Lucian, T. McNeil, S.E. Burdach, and R. Murray. 1995. Lymphopenia in interleukin (IL)-7 gene-deleted mice identifies IL-7 as a nonredundant cytokine. *J. Exp. Med.* 181:1519–1526.
10. Murray, R., T. Suda, N. Wrighton, F. Lee, and A. Zlotnik. 1989. IL-7 is a growth and maintenance factor for mature and immature thymocyte subsets. *Int. Immunol.* 1:526–531.
11. Puel, A., S.F. Ziegler, R.H. Buckley, and W.J. Leonard. 1998. Defective IL7R expression in T(-)B(+)NK(+) severe combined immunodeficiency. *Nat. Genet.* 20:394–397.
12. Noguchi, M., H. Yi, H.M. Rosenblatt, A.H. Filipovich, S. Adelstein, W.S. Modi, O.W. McBride, and W.J. Leonard. 1993. Interleukin-2 receptor gamma chain mutation results in X-linked severe combined immunodeficiency in humans. *Cell.* 73:147–157.
13. Schluns, K.S., W.C. Kieper, S.C. Jameson, and L. Lefrancois. 2000. Interleukin-7 mediates the homeostasis of naive and memory CD8 T cells in vivo. *Nat. Immunol.* 1:426–432.
14. Fry, T.J., E. Connick, J. Falloon, M.M. Lederman, D.J. Liewehr, J. Spritzler, S.M. Steinberg, L.V. Wood, R. Yarchoan, J. Zuckerman, et al. 2001. A potential role for interleukin-7 in T cell homeostasis. *Blood.* 97:2983–2990.
15. Napolitano, L.A., R.M. Grant, S.G. Deeks, D. Schmidt, S.C. De Rosa, L.A. Herzenberg, B.G. Herndier, J. Andersson, and J.M. McCune. 2001. Increased production of IL-7 accompanies HIV-1-mediated T cell depletion: implications for T cell homeostasis. *Nat. Med.* 7:73–79.
16. Bolotin, E., G. Annett, R. Parkman, and K. Weinberg. 1999. Serum levels of IL-7 in bone marrow transplant recipients: relationship to clinical characteristics and lymphocyte count. *Bone Marrow Transplant.* 23:783–788.
17. Mackall, C.L., T.J. Fry, C. Bare, P. Morgan, A. Galbraith, and R.E. Gress. 2001. IL-7 increases both thymic-dependent and thymic-independent T cell regeneration after bone marrow transplantation. *Blood.* 97:1491–1497.
18. Beq, S., M.T. Nugeyre, R. Ho Tsong Fang, D. Gautier, R. Legrand, N. Schmitt, J. Estaquier, F. Barre-Sinoussi, B. Hurtrel, R. Cheynier, and N. Israel. 2006. IL-7 induces immunological improvement in SIV-infected rhesus macaques under antiviral therapy. *J. Immunol.* 176:914–922.
19. Fry, T.J., M. Moniuszko, S. Creekmore, S.J. Donohue, D.C. Douek, S. Giardina, T.T. Hecht, B.J. Hill, K. Komschlies, J. Tomaszewski, et al. 2003. IL-7 therapy dramatically alters peripheral T cell homeostasis in normal and SIV-infected nonhuman primates. *Blood.* 101:2294–2299.
20. Storek, J., T. Gillespy III, H. Lu, A. Joseph, M.A. Dawson, M. Gough, J. Morris, R.C. Hackman, P.A. Horn, G.E. Sale, et al. 2003. Interleukin-7 improves CD4 T cell reconstitution after autologous CD34 cell transplantation in monkeys. *Blood.* 101:4209–4218.
21. Melchionda, F., T.J. Fry, M.J. Milliron, M.A. McKirdy, Y. Tagaya, and C.L. Mackall. 2005. Adjuvant IL-7 or IL-15 overcomes immunodominance and improves survival of the CD8+ memory cell pool. *J. Clin. Invest.* 115:1177–1187.
22. Li, B., M.J. Vanrooyen, and K. Jooss. 2007. Recombinant IL-7 enhances the potency of GM-CSF-secreting tumor cell immunotherapy. *Clin. Immunol.* 123:155–165.
23. Ernst, B., D.S. Lee, J.M. Chang, J. Sprent, and C.D. Surh. 1999. The peptide ligands mediating positive selection in the thymus control T cell survival and homeostatic proliferation in the periphery. *Immunity.* 11:173–181.
24. Goldrath, A.W., and M.J. Bevan. 1999. Low-affinity ligands for the TCR drive proliferation of mature CD8+ T cells in lymphopenic hosts. *Immunity.* 11:183–190.
25. Chu, Y.W., S.A. Memon, S.O. Sharrow, F.T. Hakim, M. Eckhaus, P.J. Lucas, and R.E. Gress. 2004. Exogenous IL-7 increases recent thymic emigrants in peripheral lymphoid tissue without enhanced thymic function. *Blood.* 104:1110–1119.
26. Seddiki, N., B. Santner-Nanan, J. Martinson, J. Zaunders, S. Sasson, A. Landay, M. Solomon, W. Selby, S.I. Alexander, R. Nanan, et al. 2006. Expression of interleukin (IL)-2 and IL-7 receptors discriminates between human regulatory and activated T cells. *J. Exp. Med.* 203:1693–1700.
27. Liu, W., A.L. Putnam, Z. Xu-Yu, G.L. Szot, M.R. Lee, S. Zhu, P.A. Gottlieb, P. Kapranov, T.R. Gingeras, B. Fazekas de St Groth, et al. 2006. CD127 expression inversely correlates with FoxP3 and suppressive function of human CD4+ T reg cells. *J. Exp. Med.* 203:1701–1711.
28. Rosenberg, S.A., C. Sportes, M. Ahmadzadeh, T.J. Fry, L.T. Ngo, S.L. Schwarz, M. Stetler-Stevenson, K.E. Morton, S.A. Mavroukakis, M. Morre, et al. 2006. IL-7 administration to humans leads to expansion of CD8+ and CD4+ cells but a relative decrease of CD4+ T-regulatory cells. *J. Immunother.* 29:313–319.
29. Mackall, C.L. 2000. T cell immunodeficiency following cytotoxic anti-neoplastic therapy: a review. *Stem Cells.* 18:10–18.
30. Hakim, F.T., S.A. Memon, R. Cepeda, E.C. Jones, C.K. Chow, C. Kasten-Sportes, J. Odom, B.A. Vance, B.L. Christensen, C.L. Mackall, and R.E. Gress. 2005. Age-dependent incidence, time course, and consequences of thymic renewal in adults. *J. Clin. Invest.* 115:930–939.
31. Sportes, C., N.J. McCarthy, F. Hakim, S.M. Steinberg, D.J. Liewehr, D. Weng, S. Kummar, J. Gea-Banacloche, C.K. Chow, R.M. Dean, et al. 2005. Establishing a platform for immunotherapy: clinical outcome and study of immune reconstitution after high-dose chemotherapy with progenitor cell support in breast cancer patients. *Biol. Blood Marrow Transplant.* 11:472–483.
32. Akashi, K., M. Kondo, U. von Freeden-Jeffry, R. Murray, and I.L. Weissman. 1997. Bcl-2 rescues T lymphopoiesis in interleukin-7 receptor-deficient mice. *Cell.* 89:1033–1041.
33. Hofmeister, R., A.R. Khaled, N. Benbernou, E. Rajnavolgyi, K. Muegge, and S.K. Durum. 1999. Interleukin-7: physiological roles and mechanisms of action. *Cytokine Growth Factor Rev.* 10:41–60.
34. Sereti, I., H. Imamichi, V. Natarajan, T. Imamichi, M.S. Ramchandani, Y. Badralmaa, S.C. Berg, J.A. Metcalf, B.K. Hahn, J.M. Shen, et al. 2005. In vivo expansion of CD4CD45RO-CD25 T cells expressing foxP3 in IL-2-treated HIV-infected patients. *J. Clin. Invest.* 115:1839–1847.
35. Zhang, H., K.S. Chua, M. Guimond, V. Kapoor, M.V. Brown, T.A. Fleisher, L.M. Long, D. Bernstein, B.J. Hill, D.C. Douek, et al. 2005. Lymphopenia and interleukin-2 therapy alter homeostasis of CD4+CD25+ regulatory T cells. *Nat. Med.* 11:1238–1243.
36. Ahmadzadeh, M., and S.A. Rosenberg. 2006. IL-2 administration increases CD4+ CD25(hi) Foxp3+ regulatory T cells in cancer patients. *Blood.* 107:2409–2414.
37. Kovacs, J.A., M. Baseler, R.J. Dewar, S. Vogel, R.T. Davey Jr., J. Falloon, M.A. Polis, R.E. Walker, R. Stevens, N.P. Salzman, et al. 1995. Increases in CD4 T lymphocytes with intermittent courses of interleukin-2 in patients with human immunodeficiency virus infection. A preliminary study. *N. Engl. J. Med.* 332:567–575.
38. Kovacs, J.A., S. Vogel, J.A. Metcalf, M. Baseler, R. Stevens, J. Adelsberger, R. Lempicki, R.L. Hengel, I. Sereti, L. Lambert, et al. 2001. Interleukin-2 induced immune effects in human immunodeficiency virus-infected patients receiving intermittent interleukin-2 immunotherapy. *Eur. J. Immunol.* 31:1351–1360.
39. Hassan, J., and D.J. Reen. 2001. Human recent thymic emigrants—identification, expansion, and survival characteristics. *J. Immunol.* 167:1970–1976.
40. Kaech, S.M., J.T. Tan, E.J. Wherry, B.T. Konieczny, C.D. Surh, and R. Ahmed. 2003. Selective expression of the interleukin 7 receptor identifies effector CD8 T cells that give rise to long-lived memory cells. *Nat. Immunol.* 4:1191–1198.
41. Kim, H.R., M.S. Hong, J.M. Dan, and I. Kang. 2006. Altered IL-7Ralpha expression with aging and the potential implications of IL-7 therapy on CD8+ T cell immune responses. *Blood.* 107:2855–2862.
42. Rethi, B., C. Fluur, A. Atlas, M. Krzyzowska, F. Mowafi, S. Grutzmeier, A. De Milito, R. Bellocchio, K.I. Falk, E. Rajnavolgyi, and F. Chiodi. 2005. Loss of IL-7Ralpha is associated with CD4 T cell depletion, high interleukin-7 levels and CD28 down-regulation in HIV infected patients. *AIDS.* 19:2077–2086.
43. Douek, D.C., R.A. Vescio, M.R. Betts, J.M. Brenchley, B.J. Hill, L. Zhang, J.R. Berenson, R.H. Collins, and R.A. Koup. 2000. Assessment of thymic output in adults after hematopoietic stem-cell transplantation and prediction of T cell reconstitution. *Lancet.* 355:1875–1881.

44. Broers, A.E., S.J. Posthumus-van Sluijs, H. Spits, B. van der Holt, B. Lowenberg, E. Braakman, and J.J. Cornelissen. 2003. Interleukin-7 improves T cell recovery after experimental T cell-depleted bone marrow transplantation in T cell-deficient mice by strong expansion of recent thymic emigrants. *Blood*. 102:1534–1540.
45. Mackall, C.L., T.A. Fleisher, M.R. Brown, M.P. Andrich, C.C. Chen, I.M. Feuerstein, M.E. Horowitz, I.T. Magrath, A.T. Shad, S.M. Steinberg, et al. 1995. Age, thymopoiesis, and CD4+ T-lymphocyte regeneration after intensive chemotherapy. *N. Engl. J. Med.* 332:143–149.
46. Hakim, F.T., and R.E. Gress. 2005. Reconstitution of the lymphocyte compartment after lymphocyte depletion: a key issue in clinical immunology. *Eur. J. Immunol.* 35:3099–3102.
47. Benigni, F., V.S. Zimmermann, S. Hugues, S. Caserta, V. Basso, L. Rivino, E. Ingulli, L. Malherbe, N. Glaichenhaus, and A. Mondino. 2005. Phenotype and homing of CD4 tumor-specific T cells is modulated by tumor bulk. *J. Immunol.* 175:739–748.
48. Klebanoff, C.A., L. Gattinoni, and N.P. Restifo. 2006. CD8+ T cell memory in tumor immunology and immunotherapy. *Immunol. Rev.* 211:214–224.
49. Pawelec, G., S. Koch, C. Gouttefangeas, and A. Wikby. 2006. Immunorejuvenation in the elderly. *Rejuvenation Res.* 9:111–116.
50. Sallusto, F., J. Geginat, and A. Lanzavecchia. 2004. Central memory and effector memory T cell subsets: function, generation, and maintenance. *Annu. Rev. Immunol.* 22:745–763.
51. Currier, J.R., H. Deulofeut, K.S. Barron, P.J. Kehn, and M.A. Robinson. 1996. Mitogens, superantigens, and nominal antigens elicit distinctive patterns of TCRB CDR3 diversity. *Hum. Immunol.* 48:39–51.
52. Puisieux, I., J. Even, C. Pannetier, F. Jotereau, M. Favrot, and P. Kourilsky. 1994. Oligoclonality of tumor-infiltrating lymphocytes from human melanomas. *J. Immunol.* 153:2807–2818.